

Thermodynamics of a newly constructed black hole coupled with nonlinear electrodynamics and cloud of strings

Himanshu Kumar Sudhanshu,^a Dharm Veer Singh,^{1b,d} Sudhaker Upadhyay,^{2c,d,e} Yerlan Myrzakulov,^e and Kairat Myrzakulov^e

^a*Department of Physics, J. J. College, Magadh University, Gaya, Bihar 823003, India*

^b*Department of Physics, GLA University, Mathura, Uttar Pradesh 281406, India*

^c*Department of Physics, K. L. S. College, Nawada, Magadh University, Bodh Gaya, Bihar 805110, India*

^d*School of Physics, Damghan University, PO Box 3671641167, Damghan, Iran*

^e*Department of General & Theoretical Physics, L. N. Gumilyov Eurasian National University, Astana, 010008, Kazakhstan*

*E-mail: himanshu4u84@gmail.com, veerdsingh@gmail.com,
sudhakerupadhyay@gmail.com, ymyrzakulov@gmail.com,
krmyrzakulov@gmail.com*

ABSTRACT: This paper finds an exact singular black hole solution in the presence of nonlinear electrodynamics as the source of matter field surrounded by a cloud of strings in $4D$ AdS spacetime. Here, the presence of the cloud of string, the usual Bardeen solution, becomes singular. The obtained black hole solution interpolates with the AdS Letelier black hole in the absence of both the deviation parameter and magnetic charge and interpolates with the AdS Bardeen black hole in the absence of the deviation parameter and a cloud of strings parameter. We analyse the horizon structure and thermodynamics properties, including the stability of the resulting black hole, numerically and graphically. Thermodynamical quantities associated with the black hole get modified due to the nonlinear electrodynamics and cloud of strings. Moreover, we study the effect of a cloud of strings parameter, magnetic charge and deviation parameter on critical points and phase transition of the obtained black hole where the cosmological constant is treated as the thermodynamics pressure. The critical radius increases with increasing deviation parameter values and magnetic charge values. In contrast, the critical pressure and temperature decrease with increasing deviation parameters and magnetic charge values.

¹Visiting Associate, Inter-University Centre for Astronomy and Astrophysics (IUCAA) Pune-411007, Maharashtra, India

²Visiting Associate, Inter-University Centre for Astronomy and Astrophysics (IUCAA) Pune-411007, Maharashtra, India

Contents

1	Introduction	1
2	A New Regular Black Hole Solution	3
3	Thermodynamics of NLED Black Hole in CS	8
4	$P - v$ Criticality of NLED Black Hole in CS	19
5	Results and Conclusions	24

1 Introduction

Black holes are one of the most fascinating objects proposed by Einstein's general theory of relativity (EGTR). As a theory of gravitation, in EGTR, gravitational interaction is the consequence of spacetime curvature. Elegant mathematical expressions express the geometric properties of black holes, and hence, obtaining a relevant solution for black holes from EGTR is an intricate and challenging task [1]. The Schwarzschild and Reissner-Nordström black holes are the initially well-known solutions of the EGTR without matter and with matter in spacetime, respectively. The structure of the spherically symmetric solution often has the singularity [2], which is separated by a boundary called the event horizon of a black hole. On the contrary, Einstein's field equation of general theory of relativity also has non-singular solutions of black holes known as regular black holes, which were first realised by Bardeen, who proposed a regular black hole solution without singularity but has event horizon [3] and interpreted as a solution of Einstein field equation by Ayon-Beato and Gracia in the presence of nonlinear electrodynamics (NLED) [4–6]. Though the Bardeen black hole solution is spherically symmetric, it violates the conditions of strong energy [7]. Later on, many such regular black hole solutions and their properties in spherically symmetric spacetime have been proposed [7–14]. Recently, it has been observed that regular black hole solutions in spherically symmetric spacetime violate the weak energy condition [15]. Various solutions of black hole exist in literature in which gravity is coupled with NLED sources, e.g. Born-Infeld black hole [16], Einstein Gauss-Bonnet black hole [17], charged AdS black hole [18], charged AdS Einstein Gauss-Bonnet black hole [19] and black hole in the presence of cosmic strings [20]. It has been discovered that the real linear electromagnetic field in higher energy breaks

down due to interaction with other fields. In such conditions, the best possible solution is the interaction of the gravitational field with the NLED. Also, from the perspective of the extension of EGTR, NLED sources of gravity can lead to exciting and challenging geometries, especially in the solution of regular black holes. Hence, it is essential to focus our attention on finding black hole solutions in NLED and as a consequence of this context, enormous progress has been made [21–32].

In the year 1978, Letelier proposed a new model of a black hole based on pressure-less perfect fluid, an extension of the relativistic "dust cloud" model, known as a cloud of strings (CS) [33–35], which is one-dimensional analogous to a cloud of dust having point particles. However, the whole system with CS is a closed one; its energy-momentum tensor (EMT) is conserved, which leads to applications in cosmology and astrophysics in different situations such as thermodynamics, accretion disk, quasinormal modes and several solutions have been proposed in general relativity and modified theory of gravity context in the presence of CS are reported [36–47]. Recently, a rotating black hole mimicker in the background of the CS is derived, which interpolates to regular black hole spacetime and traversable wormhole [48]. The gravitational wave echoes of black bounces surrounded by a CS are discussed to explore the effects caused by a CS in the near-horizon region [49]. Since strings are considered a fundamental component of the universe, this motivates us to investigate black hole solutions in the presence of CS.

Bekenstein and Hawking were the first to realise the black hole thermodynamics by establishing a relation between the entropy and the area of the black hole horizon [50–52]. For leading order, it is sure to the extent that entropy is proportional to the area of the black hole horizon [53–55]. For higher order, it has been studied widely [56–60]. It is always interesting to explore a new solution for gravity coupled with new sources. In this connection, this paper provides new regular black hole solutions for Einstein gravity coupled to NLED sources in the presence of CS. Further, we discuss thermodynamics, topology, Joule Thomson effect, stability, $P - v$ criticality and phase transition of this black hole [61–65].

The plan and structure of this paper are as follows. In section 2, we consider the Einstein gravity coupled to NLED in $4D$ AdS spacetime to obtain an exact black hole solution in the presence of the CS and further discuss its horizon structure for different values of parameters. We discuss the thermodynamics quantities, stability, and phase transitions in section 3. In section 4, we report this black hole's $P - v$ criticality and phase transitions analogous to the Van der Waals (VdW) fluid. We have calculated the critical values of horizon radius (or specific volume), critical pressure, critical temperature, and the universal critical compressibility factor, as well as their dependency on various parameters. Finally, in the last section, we discuss the results and final remarks on this new black hole solution and its thermodynamic properties.

For all our calculations, we adopt $(-, +, +, +)$ as metric signature and work in natural

units where $G = \hbar = c = \kappa_B = 1$.

2 A New Regular Black Hole Solution

The Einstein-Hilbert action describing Einstein's gravity coupled to NLED sources surrounded by a CS in 4D AdS spacetime [4, 20] is given by

$$\mathcal{S} = \int d^4x \sqrt{-\tilde{g}} \left[\frac{1}{2\kappa} (R - 2\Lambda) - \frac{1}{4\pi} \mathcal{L}^{NE}(F) \right] + S^{CS}, \quad (2.1)$$

where \tilde{g} is determinant of metric, R is Ricci curvature scalar and $\Lambda = -\frac{3}{l^2}$ is a cosmological constant in which l is the AdS length. $\mathcal{L}^{NE}(F)$ and S^{CS} describe Lagrangian density for NLED sources and action for CS sources, respectively, which are specified below. The Lagrangian density of NLED sources, $\mathcal{L}^{NE}(F)$ is function of $F = F_{\mu\nu}F^{\mu\nu}/4$, where $F_{\mu\nu}$ is the electromagnetic field strength tensor which is associated with the gauge potential A_μ as $F_{\mu\nu} = 2\nabla_{[\mu}A_{\nu]}$.

The $\mathcal{L}^{NE}(F)$ is the Lagrangian density of the NLED satisfying the weak energy condition ($F \ll 1$), which must be a continuous function of F such that $\partial L(F)^{NE}/\partial F \rightarrow \infty$ as $F \rightarrow \infty$ and $\mathcal{L}_F^{NE} \rightarrow 1$ as $F = 0$. Keeping this in mind, along with the regularity of spacetime, we choose

$$\mathcal{L}^{NE}(F) = \frac{F e^{-s(2g^2F)^{1/4}}}{1 + (2g^2F)^{3/4}} \left[1 + \frac{3}{s} \left(\frac{(2g^2F)^{1/2}}{1 + (2g^2F)^{3/4}} \right) \right], \quad (2.2)$$

where s is defined in terms of free parameters g and M corresponds to the magnetic charge and mass of the black hole, respectively, as $s = |g|/2M$. The Lagrangian density ($\mathcal{L}^{NE}(F)$) in the limit of $F \ll 1$ is

$$\mathcal{L}^{NE} = F + F^{\frac{3}{2}} \left(\frac{3g}{2\sqrt{2}} + \frac{s^2g}{\sqrt{2}} \right) - sF^{\frac{5}{4}}(2g^2)^{\frac{1}{4}} + F^{\frac{7}{4}} \left((2g^2)^{\frac{3}{4}} - \frac{3sg^{\frac{3}{2}}}{2^{\frac{5}{4}}} - \frac{s^3g^{\frac{3}{2}}}{32^{\frac{1}{4}}} \right) + \dots \quad (2.3)$$

In the weak field limit the Lagrangian density ($L(F)^{NE}$) goes over $L(F)^{NE} = F$, whereas in the strong-field limits, it vanishes. Here, we must emphasise that for gravity coupled to NLED with Lagrangian density, $L(F)^{NE}$, there exist spherically symmetric solutions having globally regular metric which possesses a correct weak field limit for the magnetic case only. However, one can explain the electric analogues of magnetic solutions with different Lagrangian densities (using Legendre transformation in the Hamiltonian formalism) for various ranges of radial coordinates.

The cloud of strings source is governed by the Nambu-Goto action, which is used to describe strings like object [33, 35] and is given by

$$S^{CS} = \int \sqrt{-\gamma} \mathcal{M} d\lambda^0 d\lambda^1 = \int \mathcal{M} \left(-\frac{1}{2} \Sigma^{\mu\nu} \Sigma_{\mu\nu} \right)^{\frac{1}{2}} d\lambda^0 d\lambda^1, \quad (2.4)$$

where \mathcal{M} is the dimensionless constant which characterizes the string, (λ^0, λ^1) are the time-like and spacelike coordinate parameters, respectively [66]. γ is the determinant of the induced metric, $\gamma_{ab} = \tilde{g}_{\mu\nu} \frac{\partial x^\mu}{\partial \lambda^a} \frac{\partial x^\nu}{\partial \lambda^b}$ of the strings world sheet. $\Sigma^{\mu\nu} = \epsilon^{ab} \frac{\partial x^\mu}{\partial \lambda^a} \frac{\partial x^\nu}{\partial \lambda^b}$ is bivector related to string world sheet, where ϵ^{ab} is the second rank Levi-Civita tensor which takes the non-zero values as $\epsilon^{01} = -\epsilon^{10} = 1$.

Varying the action (2.1) with respect to the metric, $\tilde{g}_{\mu\nu}$ and the gauge potential, A_μ , we can obtain the equations of motion as

$$G_{\mu\nu} + \Lambda \tilde{g}_{\mu\nu} = T_{\mu\nu}^{NE} + T_{\mu\nu}^{CS}, \quad (2.5)$$

$$\nabla_\mu \left(\frac{\partial \mathcal{L}^{NE}(F)}{\partial F} F^{\mu\nu} \right) = 0, \quad \text{and} \quad \nabla_\mu (*F^{\mu\nu}) = 0, \quad (2.6)$$

where $G_{\mu\nu}$ is the Einstein tensor, $T_{\mu\nu}^{NE}$ and $T_{\mu\nu}^{CS}$ are EMT associated with NLED and CS sources, respectively.

The EMT related to the NLED source (2.2) is given by

$$T_{\mu\nu}^{NE} = 2 \left[\frac{\partial \mathcal{L}^{NE}(F)}{\partial F} F_{\mu\sigma} F_\nu^\sigma - \tilde{g}_{\mu\nu} \mathcal{L}^{NE}(F) \right], \quad (2.7)$$

Now, to find the black hole solution with NLED sources in the presence of CS, one can consider the static spherically symmetric spacetime line element ($\kappa = c = 1$) in 4D spacetime as

$$ds^2 = -f(r)dt^2 + \frac{1}{f(r)}dr^2 + r^2 d\Omega^2, \quad \text{with} \quad f(r) = 1 - \frac{2m(r)}{r}, \quad (2.8)$$

where $d\Omega^2 = d\theta^2 + \sin^2 \theta d\phi^2$ is metric of unit 2D sphere. The metric function $f(r)$ is to be determined by solving the field equations (2.5) and (2.6).

To determine the metric function, we examine the following magnetic charge choice for Maxwell's field strength tensor $F_{\mu\nu}$

$$F_{\mu\nu} = 2\delta_{[\mu}^\theta \delta_{\nu]}^\phi Z(r, \theta). \quad (2.9)$$

Substituting ansatz (2.9) in equation of motion (2.6) and integrating, we obtain [4]

$$F_{\mu\nu} = 2\delta_{[\mu}^\theta \delta_{\nu]}^\phi h(r) \sin \theta. \quad (2.10)$$

The non-vanishing component of $F_{\mu\nu}$ is $F_{\theta\phi} = h(r) \sin \theta$ with potential $A_\phi = -h(r) \cos \theta$ [4]. Using $dF = 0$; Hence $g(r) \sin \theta dr \wedge d\theta \wedge d\phi = 0$, which conclude that $h(r) = \text{constant} = g$. Here, g is the magnetic charge. Hence, the magnetic field strength is given by

$$F_{\theta\phi} = g \sin \theta \quad \text{and} \quad F = \frac{1}{2} \frac{g^2}{r^4}. \quad (2.11)$$

Now, substituting the value of magnetic field strength, F from equation (2.11) to equation (2.2), one can obtain the Lagrangian density of NLED sources as

$$\mathcal{L}^{NE}(F) = \frac{g^2}{2r} \frac{e^{-sg/r}}{(r^3 + g^3)} \left[1 + \frac{3}{s} \left(\frac{g^2 r}{r^3 + g^3} \right) \right], \quad (2.12)$$

and using equation (2.7) and equation (2.11), the T^{NEt}_t and T^{NEr}_r components of energy momentum tensor is obtained as

$$T^{NEt}_t = T^{NEr}_r = -2\mathcal{L}^{NE}(F) = -\frac{2Me^{-k/r}}{(r^3 + g^3)} \left(\frac{k}{r} + \frac{3g^3}{r^3 + g^3} \right), \quad (2.13)$$

where $k = g^2/2M$ is known as deviation parameter and the equation (2.13) satisfy the equation of motion for NLED.

The EMT for the CS (2.4) is calculated from the definition as

$$T_{\mu\nu}^{CS} = 2 \frac{\partial}{\partial \tilde{g}_{\mu\nu}} \mathcal{M} \left(-\frac{1}{2} \Sigma^{\mu\nu} \Sigma_{\mu\nu} \right)^{1/2} = \frac{\rho \Sigma_{\alpha\nu} \Sigma_{\mu}^{\alpha}}{\sqrt{-\gamma}}, \quad (2.14)$$

where ρ is the proper density of the CS. From the conservation of law, $\nabla_{\mu} T_{\mu\nu}^{CS} = 0$, we obtain the non-vanishing components of the EMT of the CS as

$$T^{CS t}_t = T^{CS r}_r = -\frac{a}{r^2}, \quad (2.15)$$

where a is the constant known as the CS parameter.

Using the Eq. (2.8) the value of (r, r) components in equation (2.5), one get,

$$m'(r) = -\frac{3r^2}{2l^2} + \frac{a}{2} - \frac{Mre^{-k/r}}{(r^3 + g^3)} \left(k + \frac{3g^3 r}{r^3 + g^3} \right). \quad (2.16)$$

On integrating equation (2.16) with respect to r from r to ∞ , we get

$$m(r) = -\frac{r^3}{2l^2} + \frac{ar}{2} - \int_r^{\infty} \left[\frac{Mre^{-k/r}}{(r^3 + g^3)} \left(k + \frac{3g^3 r}{r^3 + g^3} \right) \right] dr + C_1. \quad (2.17)$$

Here, C_1 is the integration constant determined through condition $\lim_{r \rightarrow \infty} \left(m(r) + \frac{r^3}{2l^2} - \frac{ar}{2} \right) = M$ (mass of black hole) such that

$$C_1 = M, \quad (2.18)$$

and

$$\int_r^{\infty} \left[\frac{Mre^{-k/r}}{(r^3 + g^3)} \left(k + \frac{3g^3 r}{r^3 + g^3} \right) \right] dr = M - \frac{Mr^3}{r^3 + g^3} e^{-k/r}. \quad (2.19)$$

Substituting the value of (2.18) and (2.19) into Eq. (2.17), we get

$$m(r) = \frac{Mr^3}{r^3 + g^3} e^{-k/r} - \frac{r^3}{2l^2} + \frac{ra}{2}. \quad (2.20)$$

and the metric function for a 4D black hole with NLED sources in the presence of CS is obtained as

$$f(r) = 1 - a + \frac{r^2}{l^2} - \frac{2Mr^2 e^{-k/r}}{r^3 + g^3}. \quad (2.21)$$

The obtained regular black hole solution (2.21) is characterised by mass, M , cosmological constant as $l = \sqrt{-3/\Lambda}$, the cloud of the string parameter, a , magnetic charge, g and the deviation parameter, k , which ensure its deviation from the Bardeen black hole. For $k = g = 0$, it reduces to the Letelier solution [33], and also for $a = 0$, it corresponds to the Schwarzschild black hole solution in AdS spacetime. In the limit $r \ll 1$, the obtained black hole solution (2.21) becomes

$$f(r) = 1 - a - \frac{r^2}{l_{eff}^2} + \frac{2Mk}{g^3} \quad (2.22)$$

where $1/l_{eff}^2 = 2M/g^3 - 1/l^2$ and in the limit of $r \gg 1$ is

$$f(r) = 1 - a - \frac{2M}{r} + \frac{r^2}{l^2} \quad (2.23)$$

To study the nature of singularities structure of this black hole (2.21) at $r = 0$, it becomes essential to analyse the curvature invariants of the spacetime such as Ricci scalar, R , Ricci square, $R_{\mu\nu}R^{\mu\nu}$ and Kretshmann scalars, $R_{\mu\nu\rho\sigma}R^{\mu\nu\rho\sigma}$.

$$R = -\frac{12}{l^2} + \frac{2a}{r^2} - \frac{12Mr^2e^{-k/r}}{A^2} \left(k + 5r - \frac{3r^4}{A} \right) + \frac{2Me^{-k/r}}{A} \left(12 + \frac{6k}{r} + \frac{k^2}{r^2} \right), \quad (2.24)$$

$$\begin{aligned} R_{\mu\nu}R^{\mu\nu} &= \frac{8aMe^{-\frac{k}{r}}}{A} \left(\frac{3}{r^2} + \frac{k}{r^3} - \frac{3r}{A} \right) - \frac{12Me^{-\frac{k}{r}}}{l^2A} \left(12 - \frac{6r^2(k+5)}{A} + \frac{k(1+6r)}{r^2} + \frac{18r^6}{A^2} \right) \\ &+ \frac{2a(al^2 - 6r^2)}{l^2r^4} + \frac{2M^2e^{-2\frac{k}{r}}}{A^2} \left(\frac{324r^{12}}{A^4} - \frac{216r^8(k-r)}{A^3} + \frac{36(2k^2r^4 + 23r^6 - 12kr^4)}{A^2} \right) \\ &+ \frac{36}{l^4} - \frac{12}{A} (k^3 + 8k^2r + 24kr^2 - 30r^3) + \left(\frac{72(k+r)}{r} + \frac{32k^2}{r^2} + \frac{8k^3}{r^3} + \frac{k^4}{r^4} \right), \quad (2.25) \end{aligned}$$

$$\begin{aligned} R_{\mu\nu\rho\sigma}R^{\mu\nu\rho\sigma} &= \frac{12Me^{-k/r}}{l^2A} \left(\frac{24r^6}{A^2} - \frac{1}{A} (8kr^2 + 28r^3 - 3r^5) + \left(4 + kr - 3r^2\frac{4k^2}{3r^2} + \frac{4k}{r} \right) \right) \\ &+ \frac{9r^2}{l^4} - \frac{12}{l^2} + a^2 \left(\frac{4}{r^4} + \frac{1}{r^2} \right) - 2a \left(\frac{4}{l^2r^2} + \frac{3}{l^2} \right) + \frac{4M^2e^{-2k/r}}{A^2} \left(\frac{216}{A^3} \right. \\ &- \frac{1}{A^2} (144 + 360r^6 + 9r^8) + \frac{1}{A} (36r + 144kr^2 + 168r^3 - 6k - 18) + 6ar - 12 \\ &\left. - \frac{16k^2}{r^2} - \frac{24}{r} + k^2 - 4k^3 - 16k^2 + 9r^2 \right), \quad (2.26) \end{aligned}$$

where $A = g^3 + r^3$. Here, we see that these curvature invariants diverge in the limit $r \rightarrow 0$ in the presence of the CS parameter. This result matches with the result shown in [67]. Hence, this black hole solution (2.21) is singular everywhere in spacetime and hence, the obtained black hole solution (2.21) is singular. But in the absence of the CS parameter, the invariants are well-behaved with finite constant values at the origin, indicating the regular solution.

Now, the nature of the black hole horizon for the solution obtained in (2.21) can be determined by equations $f(r) = 0$ and $f'(r) = 0$ [68]. We can obtain the horizon of the obtained black hole solution and the degenerate horizon. The equation (2.21) is transcendental. Hence its analytic solution does not exist and thus can be solved numerically only as shown in Fig. 2 and its numerical values of the Cauchy (or inner) horizon (r_-) and the event (or outer) horizon (r_+) along with their deviation $\delta (= r_+ - r_-)$ are shown in Table 1 for different values of parameters.

As we notice from Fig. 2 and Table 1, the horizon structure of the black hole depends on the parameters a, g and k . There is no horizon radius for a value of deviation parameters $k > k_c$ or magnetic charge $g > g_c$, which is called the critical value. There exists both Cauchy horizon (r_-) and event horizon (r_+) for parameters k or g less than its critical value. For the critical value of these parameters, only the event horizon of the black hole exists. It is worth mentioning that the horizon of the black hole decreases with the increase in the value of g and k but increases with the increase in a . In addition, the critical value of the magnetic charge, g_c or the deviation parameter, k_c , increases with increasing the value of a .

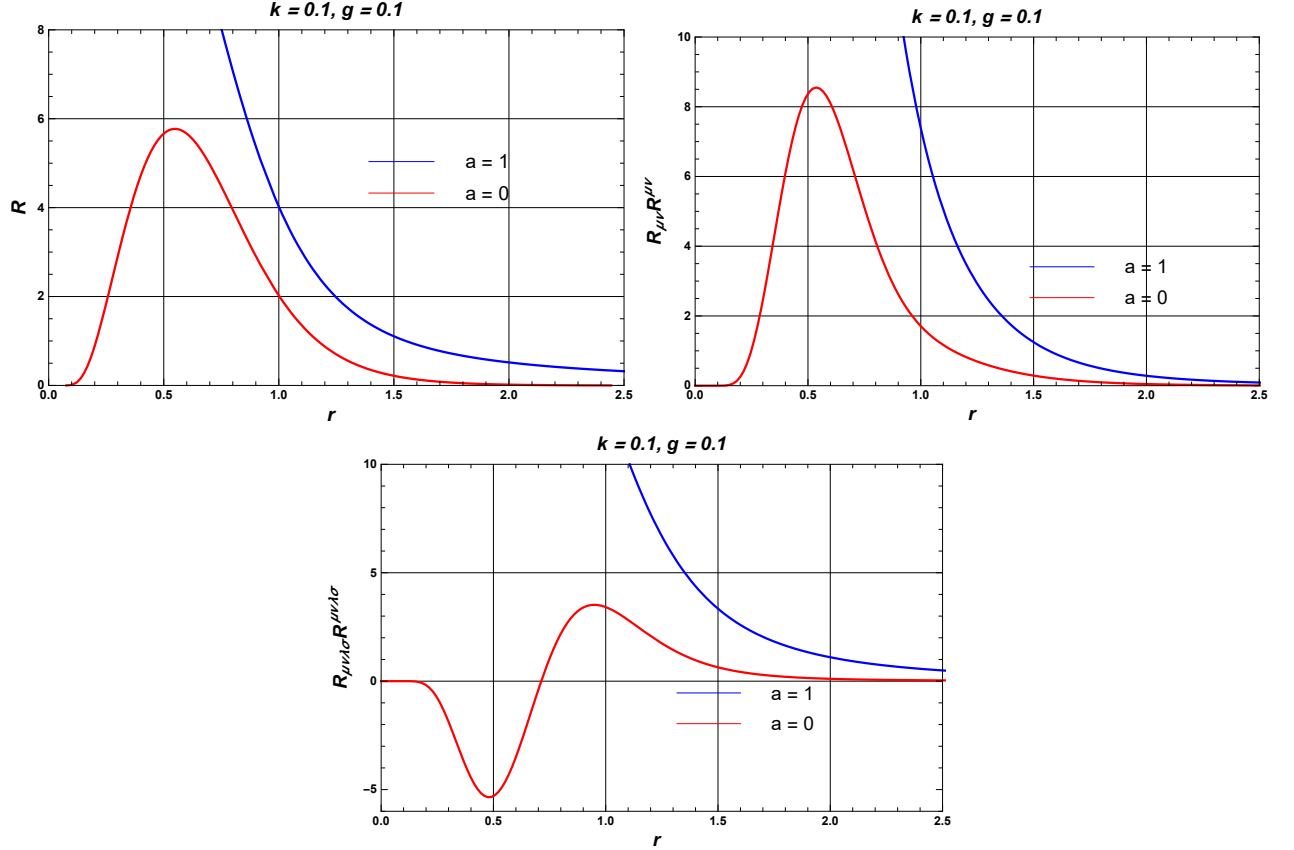


Figure 1. The Plot of curvature invariants vs radial distance with a fixed value of $k = 0.1$, $g = 0.1$ and different a with $M = 1$ and $l = 10$.

3 Thermodynamics of NLED Black Hole in CS

In this section, we study the thermodynamic properties of a $4D$ AdS black hole with NLED sources in a CS. In this connection, we discuss the thermodynamic parameters of the mass, temperature, entropy, specific heat capacity and Gibbs free energy at the event horizon for different values of parameters a , g and k of the black hole [68, 69].

The mass of the black hole, M can be evaluated from metric function (2.21) at the horizon by setting metric function $f(r)|_{r=r_+} = 0$ as

$$M = \frac{(r_+^3 + g^3) \left(1 - a + \frac{l^2}{r_+^2}\right)}{2r_+^2} e^{k/r_+}. \quad (3.1)$$

The expression represents the mass of a $4D$ AdS black hole with NLED in the CS. The mass of the obtained black hole solution (2.21) reduces to the mass of the Letelier black hole with

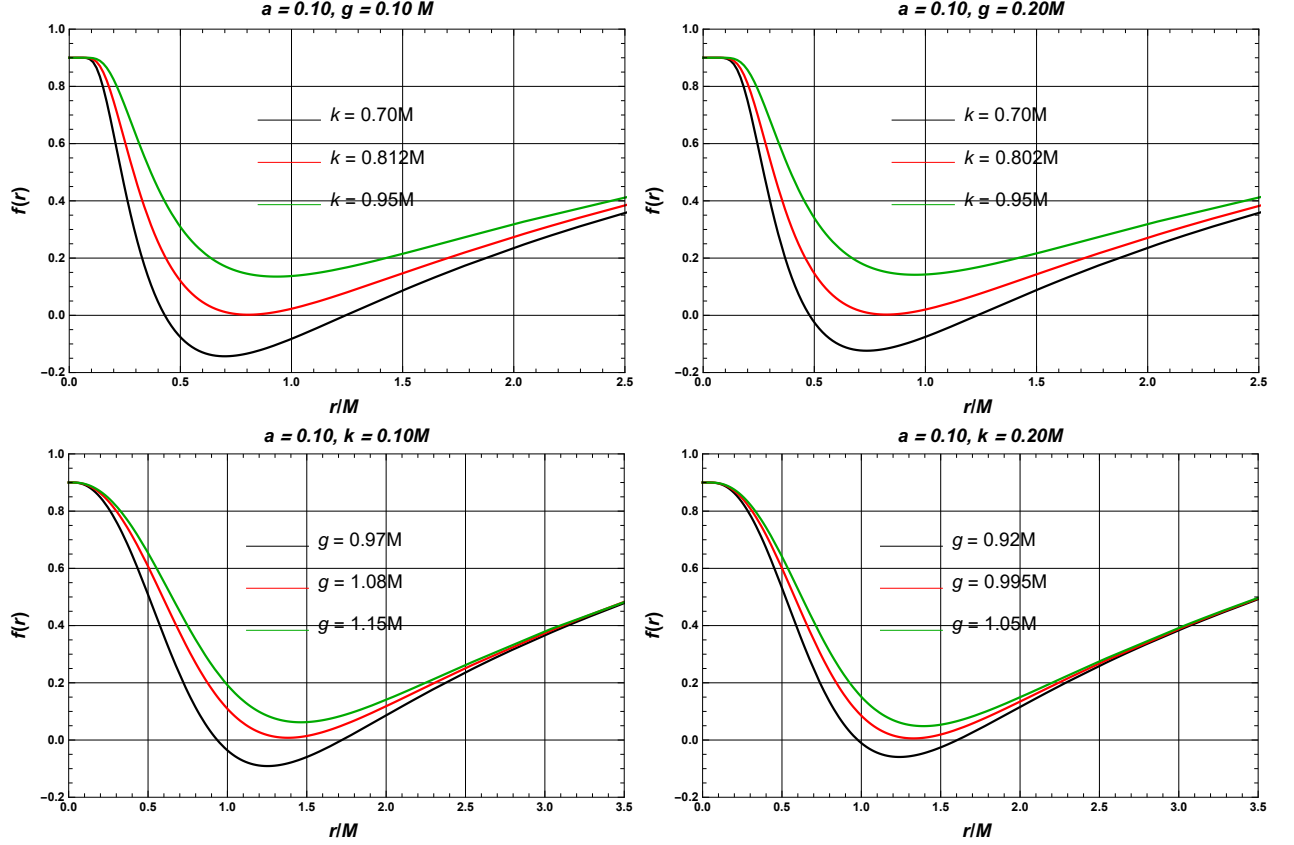


Figure 2. The Plot of metric function, $f(r)$ versus horizon radius, r of 4D NLED black hole in a CS for different value of k , g and a with $M = 1$ and $l = 10$.

CS in the absence of magnetic monopole charge, *AdS* Hayward black hole in the absence of (k, a) [26, 27] and *AdS* regular black hole in the absence of (g, a) [25]. For various values of parameters a , g , and k , the mass (M) has been plotted with horizon radius (r_+). As the radius of the black hole decreases, its mass decreases linearly, like the Schwarzschild black hole. At a particular critical horizon radius, its mass decreases to a minimum value, after which mass increases exponentially and tends to infinity (singularity) as the horizon radius approaches zero. Further, we observe that the black hole's mass increases with the value of g or k . At the same time, it decreases with an increase in the value of the CS parameter (a). It reduces to the mass of 4D *AdS* Schwarzschild black hole for vanishing the value of all the three parameters a , g and k . The minimum value of mass and its critical radius increases with the values of k and g . In contrast, it has the opposite variation for the CS parameter, a . The Hawking temperature for the regular black hole solution (2.21) can be estimated from

$a = 0.10, g = 0.10$				$a = 0.20, g = 0.10$			
k	r_-	r_+	δ	k	r_-	r_+	δ
0.20	0.087	1.923	1.837	0.20	0.083	2.153	0.901
0.40	0.167	1.702	0.619	0.40	0.158	1.943	1.785
0.60	0.310	1.426	1.116	0.60	0.280	1.693	1.413
0.80	0.682	0.930	0.248	0.80	0.501	1.352	0.851
$k_c = 0.810$		0.803		$k_c = 0.909$		0.895	

$a = 0.10, k = 0.10$				$a = 0.20, k = 0.10$			
g	r_-	r_+	δ	g	r_-	r_+	δ
0.20	0.104	2.021	1.917	0.20	0.099	2.248	2.148
0.40	0.230	2.008	1.778	0.40	0.217	2.237	2.020
0.60	0.403	1.969	1.566	0.60	0.375	2.208	1.833
0.80	0.639	1.883	1.244	0.80	0.581	2.145	1.564
$g_c = 1.070$		1.371		$g_c = 1.203$		1.524	

Table 1. For different values of parameters a , g and k with $M = 1$ and $l = 10$, Cauchy horizon (r_-), event horizon (r_+) and their deviation $\delta (= r_+ - r_-)$ has been tabulated numerically for 4D NLED black hole in CS.

the standard formula

$$T_+ = \frac{1}{4\pi} f'(r)|_{r=r_+}, \quad (3.2)$$

where $f'(r)$ denotes the differentiation of metric function (2.21) with respect to r , and in our case it is obtained as

$$T_+ = \frac{1}{4\pi l^2 r_+^2} \left[2r_+^3 - \frac{(r_+^2 - (a-1)l^2)(r_+^3(k-r_+) + g^3(k+2r_+))}{(r_+^3 + g^3)} \right]. \quad (3.3)$$

The Hawking temperature, T_+ (3.3), is characterized by the black hole parameters a , g and k and on cosmological length, l . It is clear from the expression that it reduces to the temperature of 4D AdS Schwarzschild black hole in the limit all the three parameters a , g and k tends to zero and it reduces to

$$T_+^{Swzc} = \frac{1}{4\pi} \left(\frac{1}{r_+} + \frac{3}{l^2} \right). \quad (3.4)$$

We plot the temperature (3.3) of the 4D AdS black hole with NLED in the CS in Fig. 3 for different values of g , k and CS parameters (a) to analyse the functioning of temperature with the horizon radius of this black hole. The temperature of the obtained black hole

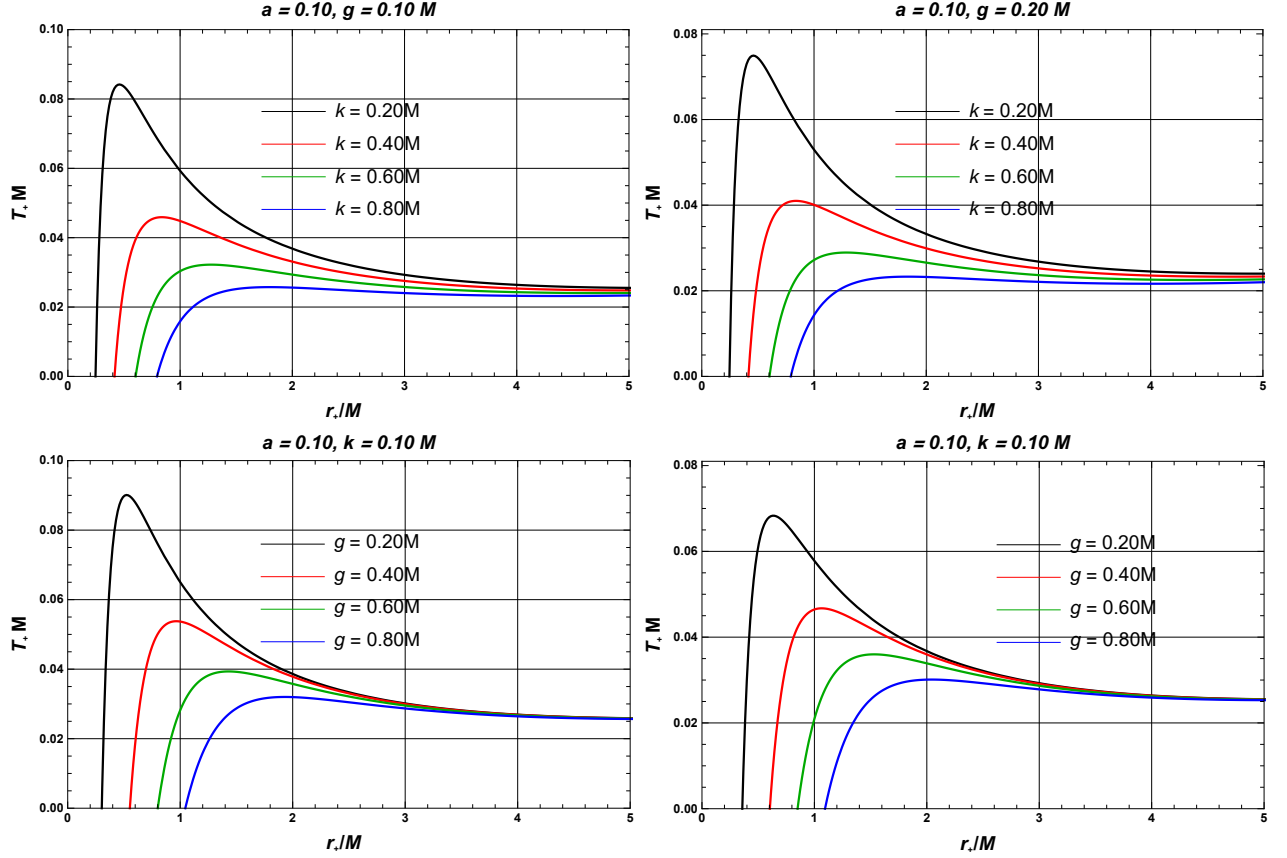


Figure 3. Plot of Hawking temperature T_+ versus horizon radius, r_+ of 4D NLED black hole in a CS for different value of k , g and a with $l = 10$.

solution (2.21) reduces to the temperature of the Letelier black hole with CS in the absence of magnetic monopole charge, *AdS* Hayward black hole in the absence of (k, a) [26, 27] and *AdS* regular black hole in the absence of (g, a) [25]. From the plot, we observe that the effect of g , k or a is more significant in the case of small black holes, and for the larger horizon region, it coincides with that of Schwarzschild black hole. The temperature of this regular black hole first increases sharply to attain a maximum value, T_+^{max} for a particular horizon radius, r_+^m and then decreases exponentially with an increase in horizon radius, r_+ and finally, in the region of larger black holes, it corresponds to temperature (3.4) of 4D *AdS* Schwarzschild black hole (T_+^{Swzc}). The maximum of Hawking temperature, T_+^{max} and its corresponding horizon radius, r_+^m have been computed numerically for the different values of g , k and CS parameters (a) as shown in Table 2. Here, we observe that the value of maximum temperature, T_+^{max} , increases and its corresponding horizon radius, r_+^m , decreases with a decrease in the value of parameters a , g or k .

$a = 0.10$								
	$g = 0.10$		$g = 0.20$		$g = 0.30$		$g = 0.40$	
k	r_+^m	T_+^{max}	r_+^m	T_+^{max}	r_+^m	T_+^{max}	r_+^m	T_+^{max}
0.10	0.315	0.135	0.524	0.090	0.742	0.067	0.965	0.054
0.20	0.459	0.084	0.635	0.068	0.843	0.056	1.064	0.047
0.30	0.638	0.059	0.772	0.054	0.963	0.047	1.177	0.041
0.40	0.837	0.046	0.936	0.043	1.103	0.040	1.307	0.036

$a = 0.20$								
	$g = 0.10$		$g = 0.20$		$g = 0.30$		$g = 0.40$	
k	r_+^m	T_+^{max}	r_+^m	T_+^{max}	r_+^m	T_+^{max}	r_+^m	T_+^{max}
0.10	0.315	0.120	0.524	0.080	0.743	0.060	0.967	0.048
0.20	0.460	0.075	0.635	0.061	0.845	0.050	1.067	0.042
0.30	0.639	0.053	0.774	0.048	0.966	0.042	1.181	0.037
0.40	0.839	0.041	0.939	0.039	1.108	0.036	1.313	0.032

Table 2. For different values of parameters a, g and k with $l = 10$, maximum value of Hawking temperature, T_+^{max} and its corresponding horizon radius, r_+^m have been tabulated numerically for $4D$ NLED black hole in CS.

Now, let's focus on the other most crucial thermodynamic quantity, the entropy of the black hole, by considering the first law of thermodynamics. Being a thermodynamic system, the black hole must follow the first law of thermodynamics, defined as

$$dM = T_+ dS_+ + \Phi_g dg + V_+ dP_+, \quad (3.5)$$

where S_+ is the entropy of the black hole and Φ_g is the potential for the magnetic charge, g . The thermodynamic pressure, P_+ and its conjugate thermodynamic volume, V_+ , of the black hole is given as

$$P_+ = -\frac{\Lambda}{8\pi} = \frac{3}{8\pi l^2}, \quad (3.6)$$

$$V_+ = \frac{4}{3}\pi r_+^3. \quad (3.7)$$

For the values of mass, M (3.1) and the temperature, T_+ (3.3), using the first law of thermodynamics (3.5) of BH, we can compute the entropy of the black hole from the relation,

$S_+ = \int \frac{1}{T_+} \left(\frac{\partial M}{\partial r_+} \right) dr_+$ as

$$S_+ = \pi \left[\frac{e^{k/r_+}}{k} (kr_+(k+r_+) - 2g^3) - k^2 \text{Ei} \left(\frac{k}{r_+} \right) \right], \quad (3.8)$$

where ‘‘Ei’’ is the exponential integral function. Here, we find that entropy does not depend on the CS parameters (a). Here, entropy does not follow the usual entropy area law of a black hole, $S_+ = \frac{A}{4}$, (where $A = 4\pi r_+^2$ is the area of the event horizon) in the presence of a magnetic charge, g and the deviation parameter, k . However, in the limit of parameters g and k tends to zero, we obtain the usual entropy area law as

$$S_+^{Swzc} = \pi r_+^2 = \frac{A}{4}, \quad (3.9)$$

which follows the standard Bekenstein-Hawking area law and exactly matches the entropy of the four-dimensional Schwarzschild black hole.

Now, we also checked the expression for Hawking temperature evaluated from the first law of thermodynamics (3.5) as $T_H = \left(\frac{\partial M}{\partial S} \right)$ and found to agree with the one obtained in (3.3) for a fixed value of magnetic charge ($dg = 0$). Hence, our solution for this black hole follows the first law of thermodynamics for the fixed value of the magnetic charge.

It has been demonstrated by Wald [70] that the entropy of a black hole obeys the area law, but in the case of regular black holes, one doesn't get the usual area form using the first law of thermodynamics. The deviation of the entropy (3.8) relies on the general structure of the EMT of matter fields for regular black holes. The mass term is modified in the presence of NLED with an extra factor. The modified mass is [68, 69]

$$d\mathcal{M} = \left(1 + 4\pi \int_{r_+}^{\infty} r_+^2 \frac{\partial T_t^t}{\partial M} dr_+ \right) dM = \mathcal{C}(M, g, r_+) dM. \quad (3.10)$$

The $\mathcal{C}(M, g, r_+)$ is the correction term. The modified first law of black hole thermodynamics is

$$d\mathcal{M} = T_+ dS_+ + \Phi_g dg + V_+ dP_+, \quad (3.11)$$

the conventional form of the first law gets modified with an extra factor [71]

$$\mathcal{C}(M, g, r_+) dM = T_+ dS + \Phi_g dg + V_+ dP_+, \quad (3.12)$$

where T_+ is the Hawking temperature and $\mathcal{C}(M, g, r_+)$ is

$$\mathcal{C}(M, g, r_+) = 1 + 4\pi \int_{r_+}^{\infty} r_+^2 \frac{\partial T_t^t}{\partial M} dr_+. \quad (3.13)$$

We recover the conventional form of the first law of black hole thermodynamics when the factor $\mathcal{C}(M, r_+) = 1$, as the EMT does not depend upon mass. Since any black hole has temperature, it can be seen as a thermodynamic system. Thus, the conventional thermodynamic laws must be satisfied. We have two choices to connect Eq. (3.12) with the first law of thermodynamics. We know that $\delta E = T\delta S$ then the $E \rightarrow M$ and the entropy becomes

$$\delta S_+ = \mathcal{C}(M, g, r_+) \delta M. \quad (3.14)$$

Following this modified first law of thermodynamics (3.14), the obtained entropy (3.8) of this regular black hole solution follows the usual area law (3.9) of black hole mechanics.

To analyse the behaviour of entropy (3.8) with the horizon radius of this 4D AdS black hole with NLED sources in the CS, we plot it in Fig. 4 for different values of g and k . From the plot, we see that the entropy of a black hole increases with the value of k while it has the opposite variation for g . Further, we observe that entropy is collinear in the region of this black hole's large horizon radius compared to that of the Schwarzschild black hole.

Now, to understand the thermodynamic stability of this black hole, we first study the nature of its specific heat capacity (C_+) to appreciate its local stability since the negative and positive signatures of the heat capacity define the unstable and the stable thermodynamical system of the black hole, respectively.

The specific heat capacity C_+ for the black hole can be obtained from the relation $C_+ = \left(\frac{\partial M}{\partial T_+}\right) = \left(\frac{\partial M}{\partial r_+}\right) \left(\frac{\partial r_+}{\partial T_+}\right)$, by using the expression for temperature and entropy from the equations. (3.3) and (3.8), respectively as

$$C_+ = \frac{2\pi (g^3 + r_+^3)^2 [g^3 (k (\xi - r_+^2) + 2\xi r_+) + r_+^3 (k (\xi - r_+^2) + 3r_+^3 - \xi r_+)] e^{k/r_+}}{2g^3 r_+^4 (6r_+^3 - 5\xi r_+ - 2k\xi) + r_+^7 (3r_+^3 + \xi r_+ - 2k\xi) - 2g^6 \xi r_+ (k + r_+)}, \quad (3.15)$$

where $\xi = (a - 1)l^2$.

From the expression of the specific heat capacity (3.15), it is clear that for the 4D AdS black hole with NLED sources in the CS, the heat capacity was found to depend on all parameters a , g , k and l . In the limit of a , g and k tends to zero, we obtain the expression of the heat capacity as

$$C_+^{Swzc} = 2\pi r_+^2 \left(\frac{3r_+^2 + l^2}{3r_+^2 - l^2} \right), \quad (3.16)$$

which is the expression for the heat capacity of the 4D Schwarzschild black hole in AdS spacetime. The heat capacity of the obtained black hole solution (2.21) reduces to the heat capacity of the Letelier black hole with CS in the absence of magnetic monopole charge, AdS Hayward black hole in the absence of (k, a) [26, 27] and AdS regular black hole in the absence of (g, a) [25].

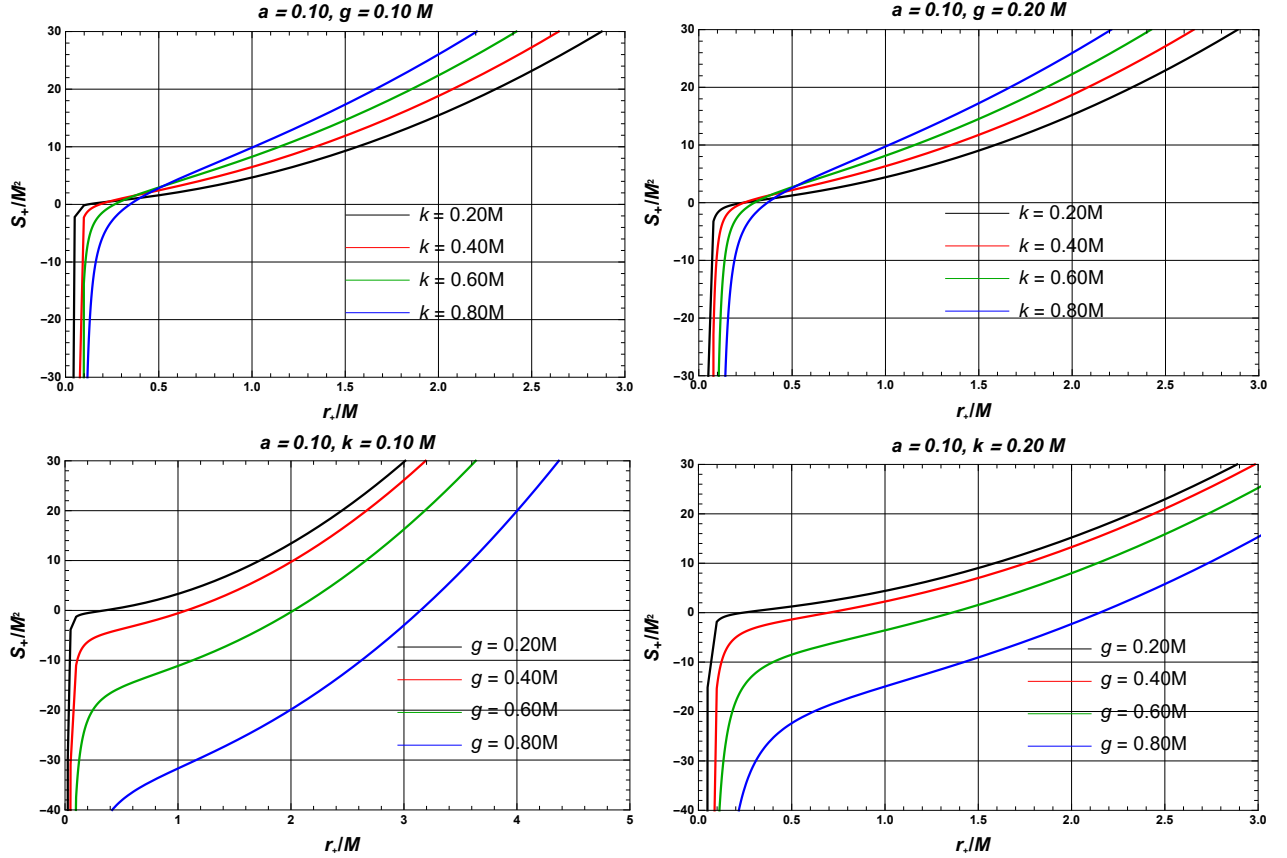


Figure 4. Plot of entropy, S_+ versus horizon radius, r_+ of 4D NLED black hole in a CS for different value of k and g .

It is clumsy to point out the signature of the heat capacity of this regular black hole from its expression. Hence, we plot the heat capacity with the horizon radius in Fig. 5 by fixing the parameters a , g and k . For different values of parameters, the heat capacity in all the cases shows asymptotic behaviour and is found to be discontinuous at a particular horizon radius, say at $r_+ = r_{h1}$ and $r_+ = r_{h2}$. For the region $r_+ < r_{h1}$ and $r_+ > r_{h2}$, the specific heat is found to have a positive value, i.e. $C_+ > 0$ and hence the black hole is thermodynamically stable. In contrast, it is thermodynamically unstable for the region $r_{h1} < r_+ < r_{h2}$ as specific heat has a negative value, i.e. $C_+ < 0$. The divergence of heat capacity at horizon radius $r_+ = r_{h1}$ and $r_+ = r_{h2}$ resembles the second-order phase transition between stable and unstable phases of the black hole when it changes size from more minor to larger or vice versa.

For further analysis, we have numerically computed the values of the particular horizon radius r_{h1} and r_{h2} along with the horizon region between these (unstable black hole region),

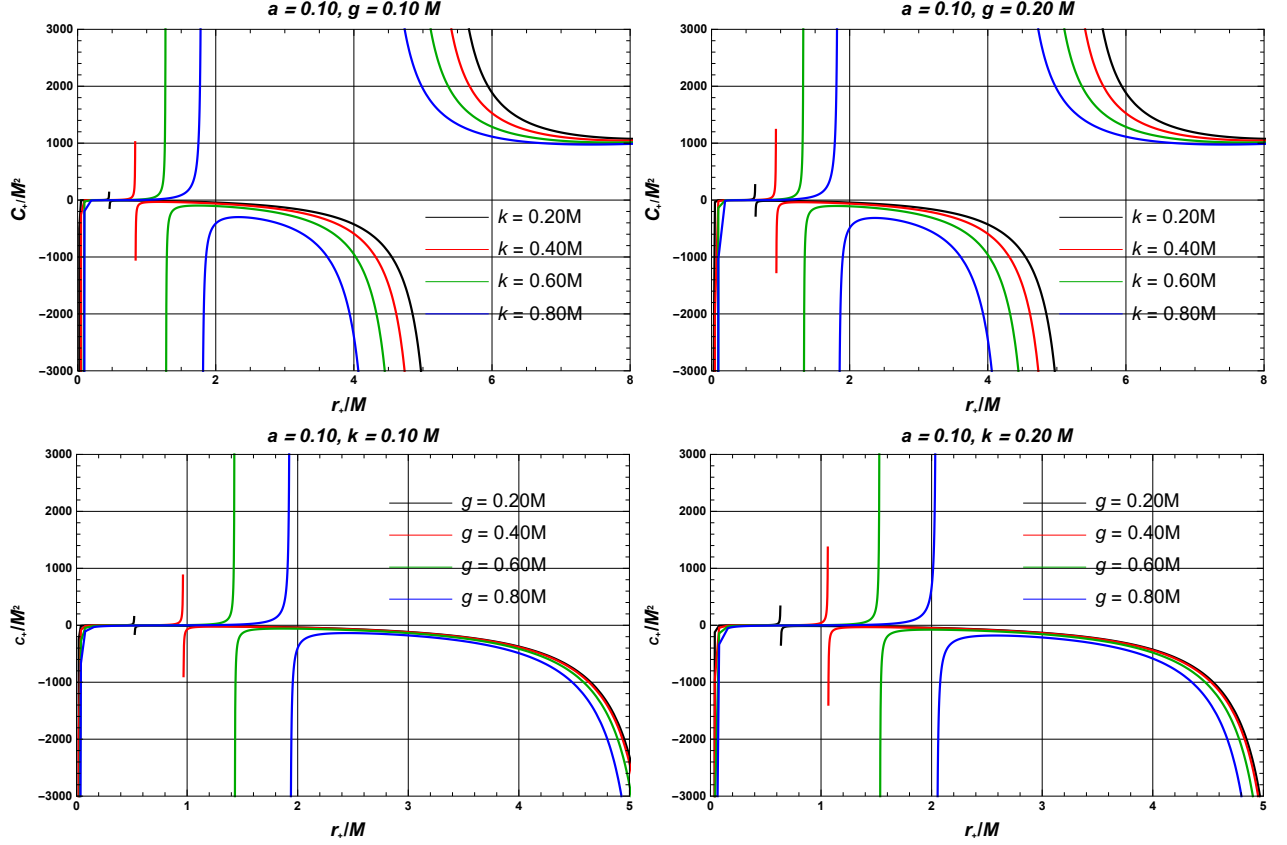


Figure 5. The Plot of heat capacity, C_+ versus horizon radius, r_+ of 4D NLED black hole in a CS for different value of k , g and a with $l = 10$.

$\Delta = (r_{h2} - r_{h1})$ as shown in Table 3 for different values of magnetic charge, g , deviation parameter, k and the CS parameters, a . As the values of these parameters increase, the particular horizon radius r_{h1} and r_{h2} increases and decreases, respectively. Consequently, the region between this horizon radius, Δ , decreases. Hence, as the value of black hole parameters a , g and k increases, the unstable region (negative heat capacity) of a black hole, Δ , reduces, i.e. the stability of a black hole increases for NLED sources in the presence of a CS.

Further, to understand the global thermal stability of the black hole system, Gibbs free energy, G_+ , plays one of the crucial roles in a thermodynamically stable system of the black hole $G_+ \leq 0$. The Gibbs free energy of the black hole can be computed from the standard relation, $G_+ = M - T_+ S_+$ by using the expression of mass, temperature and entropy from equations (3.1), (3.3) and (3.8), respectively as

$a = 0.10$							
$k = 0.10$				$g = 0.10$			
g	r_{h1}	r_{h2}	Δ	k	r_{h1}	r_{h2}	Δ
0.20	0.524	5.372	4.849	0.20	0.459	5.265	4.806
0.40	0.965	5.358	4.393	0.40	0.837	5.022	4.185
0.60	1.430	5.317	3.888	0.60	1.277	4.732	3.455
0.80	1.931	5.233	3.302	0.80	1.797	4.356	2.559

$a = 0.20$							
$k = 0.10$				$g = 0.10$			
g	r_{h1}	r_{h2}	Δ	k	r_{h1}	r_{h2}	Δ
0.20	0.524	5.059	4.535	0.20	0.460	4.951	4.491
0.40	0.967	5.042	4.075	0.40	0.839	4.704	3.865
0.60	1.436	4.996	3.560	0.60	1.287	4.404	3.117
0.80	1.949	4.898	2.948	0.80	1.836	3.999	2.163

Table 3. For different values of parameters a, g and k with $l = 10$, particular horizon radius (r_{h1}) and (r_{h2}) along with unstable region, Δ has been tabulated numerically for 4D NLED black hole in CS.

$$G_+ = \frac{[k(r_+^3 + g^3)(r_+^2 - \xi)e^{k/r_+}] - \left[\left(\frac{r_+^3 - 2g^3}{r_+^3 + g^3}\right)r_+ + 2r_+^3 - k\right] \left[(k^2r_+ + kr_+^2 - 2g^3)e^{k/r_+} - k^3\text{Ei}\left(\frac{k}{r_+}\right)\right]}{4l^2r_+^2}. \quad (3.17)$$

In the limit of parameters a, g , and k tends to zero, we obtain the Gibbs free energy as

$$G_+^{Swzc} = \frac{1}{4} \left(1 - \frac{r_+^2}{l^2}\right) r_+, \quad (3.18)$$

which is the expression of Gibbs free energy for 4D Schwarzschild black hole in AdS spacetime. The Gibbs free energy of the obtained black hole solution (2.21) reduces to the Gibbs free energy of the Letelier black hole with CS in the absence of magnetic monopole charge, AdS Hayward black hole in the absence of (k, a) [26, 27] and AdS regular black hole in the absence of (g, a) [25].

For the analysis of the global stability of the 4D AdS black hole with NLED sources in the presence of a CS, Gibbs free energy is plotted in Fig. 6 with horizon radius for different values of a CS parameter (a), g and k .

From the plot Fig. 6, we see that the effect of a CS parameter a, g or k is more significant for small black holes. In the variation of g or k for a fixed value of a , Gibbs free energy

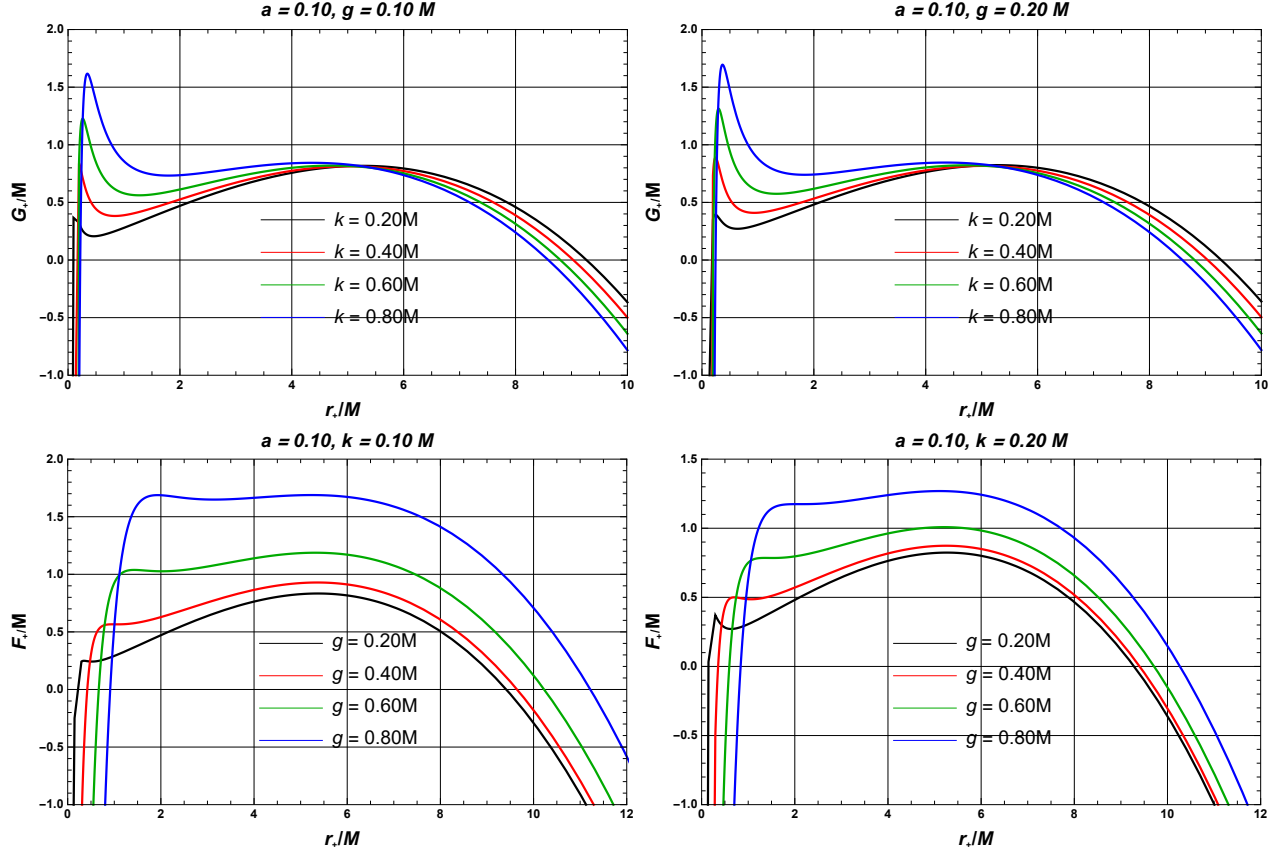


Figure 6. Plot of Gibbs free energy, G_+ versus horizon radius, r_+ of 4D NLED black hole in a CS for different value of k , g and a with $l = 10$.

attains a maximum positive value ($G_+^{max} > 0$) and then it drops to a local minimum value, then increases to a local maximum value and remains positive, after that it attains the local maximum value, from where its slope turns negative and Gibbs free energy becomes negative to coincide with the 4D AdS Schwarzschild black hole in large black hole region.

Here, we observe that the Gibbs free energy attains local minimum and local maximum values at the particular horizon radius, r_{h1} and r_{h2} , respectively, at which the specific heat capacity (3.15) flip its sign (see Table 3 and Fig. 5). For the horizon radius, $r_+ > r_{h1}$, the slope of the Gibbs free energy has an increasing function (positive slope) with the horizon radius and achieves the local maximum value at the horizon radius $r_+ = r_{h2}$, after which its slope turns negative. Hence, it provides the theory of the usual Hawking-Page phase transition of the black hole. For a particular case of $a = 0.10, g = 0.10$ and $k = 0.60$, these have been depicted in Fig. 7. Further, it is observed that as the values of parameters increase, a, g and k increase, the horizon region between the local minimum and local maximum

decreases, and hence, similar to the case of specific heat capacity, the unstable region of a black hole, Δ reduces and therefore stability region of this NLED black hole in the presence of CS increase.

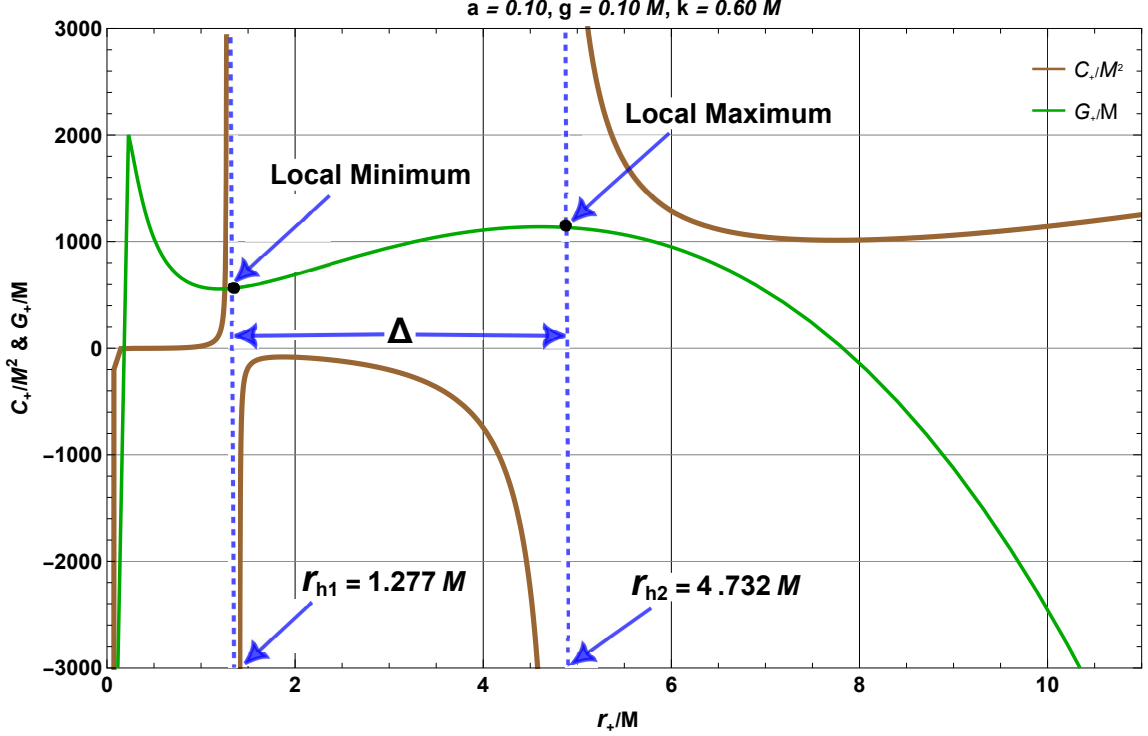


Figure 7. Depiction of Hawking-Page phase transition of 4D NLED black hole in a CS for $a = 0.10, g = 0.10M$ and $k = 0.60M$ with $l = 10$, showing local minimum and local maximum at horizon radius $r_+ = r_{h1}$ and $r_+ = r_{h2}$, respectively (Graph not to scale in vertical axis).

4 $P - v$ Criticality of NLED Black Hole in CS

In this section, we study the critical behaviour and phase transition of the 4D AdS black hole solution with NLED sources in the presence of CS in the extended phase space analogous to the VdW fluid. Since in the extended thermodynamics, the negative cosmological constant ($\Lambda < 0$) induces the thermodynamic pressure of the black hole as shown in equation (3.6) and the thermodynamic volume (3.7) is conjugate to the pressure, hence it can be interpreted as the change in mass of the black hole under the variation of the pressure having fixed horizon area as $V_+ = \left(\frac{\partial M}{\partial P_+} \right)_{S_+}$. The mass of the black hole (M) is then equivalent to the enthalpy of the black hole system.

The equation of the state for this black hole thermodynamic system can be obtained by putting the value of l from equation (3.6) in equation (3.3) as

$$P_+ = \frac{3}{8\pi r_+^2} \left[\frac{r_+^3(k - ak + r_+(-1 + a + 4\pi r_+ T_+)) + g^3(k - ak + 2r_+(1 - a + 2\pi r_+ T_+))}{3r_+^4 - k(r_+^3 + g^3)} \right], \quad (4.1)$$

and comparing the equation (4.1) with the VdW equation of the fluid [72]

$$P = \frac{T}{v - \beta} - \frac{\alpha}{v^2} \approx \frac{T}{v} + \frac{\beta T - \alpha}{v^2} + O(v^{-3}), \quad (4.2)$$

where v is the specific volume of the fluid and constants α and β (both > 0) represent the measure of the attraction between molecules and the size of the molecules in the fluid, respectively. We obtain the specific volume of this black hole thermodynamics system as [57]

$$v = 2 \left(\frac{r_+^4}{r_+^3 + g^3} - \frac{k}{3} \right). \quad (4.3)$$

In the limit g and k tend to zero, the specific volume becomes $v = 2r_+$.

The critical components of temperature, T_c pressure, P_c and specific volume, v_c or horizon radius, r_c , can be determined from the condition of inflection point at critical components P_c and v_c by satisfying the following conditions

$$\left(\frac{\partial P_+}{\partial r_+} \right) = 0 \quad \text{and} \quad \left(\frac{\partial^2 P_+}{\partial r_+^2} \right) = 0. \quad (4.4)$$

Using the critical point conditions (4.4) in the equation of state (4.1), one gets the following equation.

$$\frac{3(a - 1) (4g^6(6k + 5r_+) + g^3 r_+^3(9k + 28r_+) + r_+^6(3k - r_+))}{4\pi r_+^4 (4g^3 + r_+^3) (g^3 k + r_+^3(k - 3r_+))} = 0 \quad (4.5)$$

The critical point horizon radius, r_c , can be obtained by solving the equation (4.5). However, one can't solve it analytically, but the critical radius r_c (or specific volume from equation (4.3)), critical temperature T_c and critical pressure P_c can be computed numerically for the specific values of parameters a , g and k of this 4D AdS black hole with NLED sources in the CS as shown in Table 4. The universal ratio, critical compressibility factor, Z_c , which describes the deviation of the real thermodynamic system from its behaviour as an ideal gas, is calculated by relation $Z_c = \frac{P_c v_c}{T_c}$.

To analyse the behaviour of black hole pressure with the horizon radius at the isotherm, we plot the expression of pressure (3.6) for different values of parameters a , g and k as shown in Fig. 8.

$a = 0.10, g = 0.10$					$a = 0.20, g = 0.10$				
k	r_c	P_c	T_c	Z_c	k	r_c	P_c	T_c	Z_c
0.20	0.669	0.029	0.109	0.318	0.20	0.669	0.026	0.096	0.318
0.40	1.221	0.008	0.057	0.310	0.40	1.221	0.007	0.051	0.310
0.60	1.809	0.004	0.038	0.308	0.60	1.809	0.003	0.034	0.308
0.80	2.405	0.002	0.029	0.308	0.80	2.405	0.002	0.026	0.308

$a = 0.10, k = 0.10$					$a = 0.20, k = 0.10$				
g	r_c	P_c	T_c	Z_c	g	r_c	P_c	T_c	Z_c
0.20	0.737	0.032	0.122	0.357	0.20	0.737	0.028	0.108	0.357
0.40	1.341	0.010	0.072	0.368	0.40	1.341	0.009	0.064	0.368
0.60	1.951	0.005	0.051	0.372	0.60	1.951	0.004	0.045	0.372
0.80	2.562	0.003	0.039	0.374	0.80	2.562	0.003	0.035	0.374

Table 4. The critical temperature T_c , critical pressure P_c and critical compressibility factor, Z_c for different values of parameters a , g and k has been tabulated numerically for 4D NLED black hole with CS.

From Table 4 and Fig. 8, it is clear that the critical horizon radius, r_c and hence critical specific volume, v_c , increases with the increase in the values of g or k , but found to be independent of CS parameter (a). Though the universal compressibility ratio, Z_c , increases with an increase in the value of the parameter magnetic charge, g and decreases with an increase in the value of the deviation parameter, k , it is found to be independent of a CS parameter, a . The universal ratio, Z_c , is found to be analogous to that of the VdW fluid, for which its universally accepted value is 0.375. It means that the deviation parameter and magnetic charge behaviour are opposite on the Z_c . Both critical pressure and critical temperature decrease with increasing values of parameters a , g , and k . It is important to note that the critical radius (or critical specific volume) of the black hole thermodynamic system increases with the deviation parameter (k) and the magnetic charge (g). Small black hole and large black hole are stable. However, intermediate black hole is unstable since the heat capacity C_+ is negative (see Fig. 3). When $T_+ < T_*$, the small black hole is obtained, and $T_+ > T_*$ corresponding to a large black hole due to small free energy, where T_* is the transition temperature, which are 0.081, 0.042 for $k = 0.2$ and $k = 0.4$ with fixed value of $a = g = 0.1$, respectively. We can transit from one phase to another phase at critical temperature due to the same free energy.

Now, to study the phase structure of the black hole thermodynamic system, we plot the Gibbs free energy (3.17) versus temperature (3.3) for $P < P_c$, $P = P_c$ and $P > P_c$ with the variation of the magnetic charge (g), k and the CS parameter (a) of this black hole solution

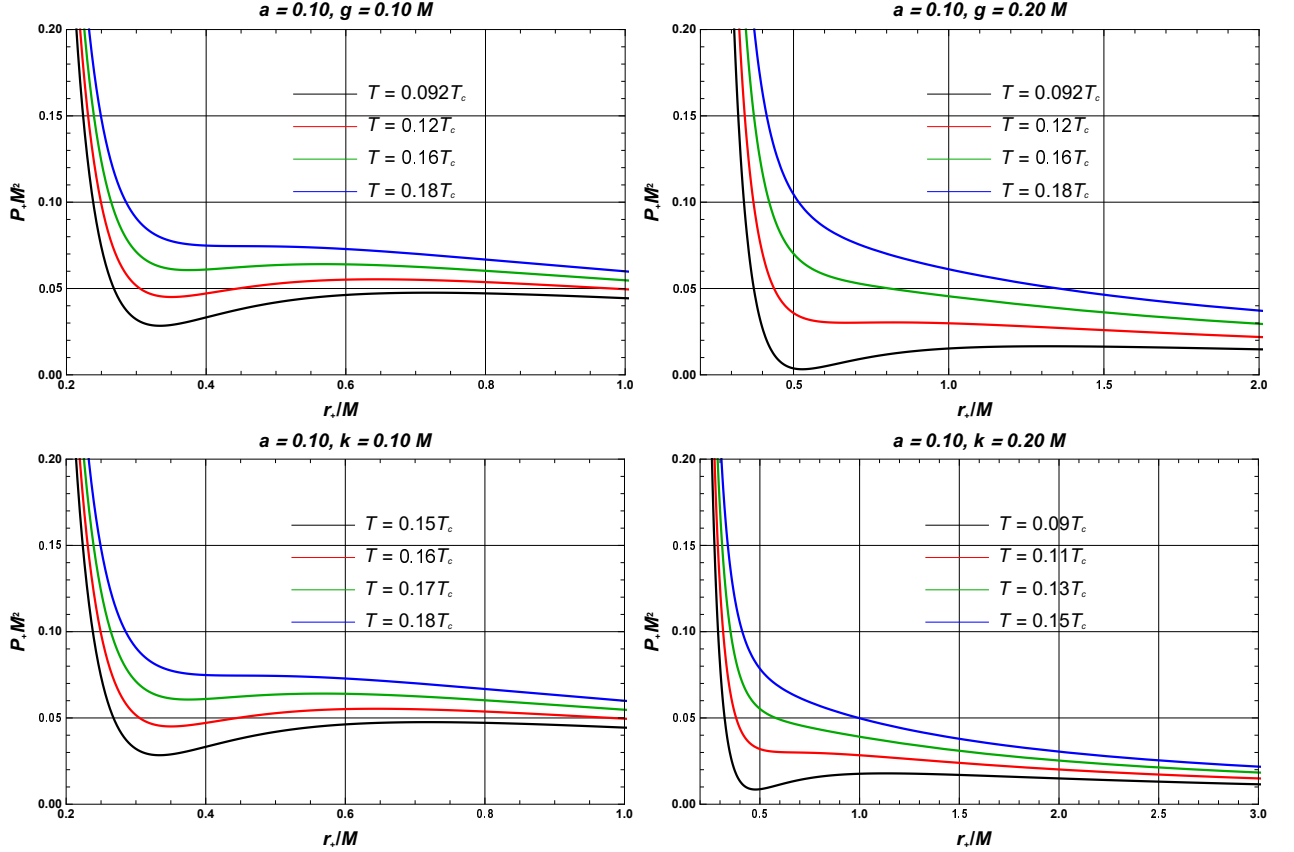


Figure 8. Plot of pressure, P_+ versus horizon radius, r_+ at the corresponding critical temperature, T_c of 4D NLED black hole in a CS for different value of k , g and a .

as shown in Fig. 9. The Gibbs free energy, G_+ , which analyses the phase transition of the black hole thermodynamic system analogous to the VdW fluid phase transition, shows variation with parameters a , g and k on the phase structure of the black hole system. In $G_+ - T_+$ plots, the appearance of characteristic swallow tail shows that the obtained values are critical for phase transition. In Fig. 9, we can see that the swallow tail shape exists when $P < P_c$ for the first order phase transition and $P = P_c$ for the second order phase transition. There is no phase transition when thermodynamic pressure is larger than the critical pressure P_c . The black hole transits from one phase to another due to the same free energy; the corresponding temperature is the transition temperature. The sub-critical isobar is the region where the phase transition takes place. It is noted that the Gibbs free energy of two phases is a decreasing function of CS parameter (a) and deviation parameter (k).

In the G_+ vs T_+ plots in Fig. 9, the characteristic swallow tail indicates the critical values where the phase transition occurs. From the plot Fig. 9, we observe that the swallow

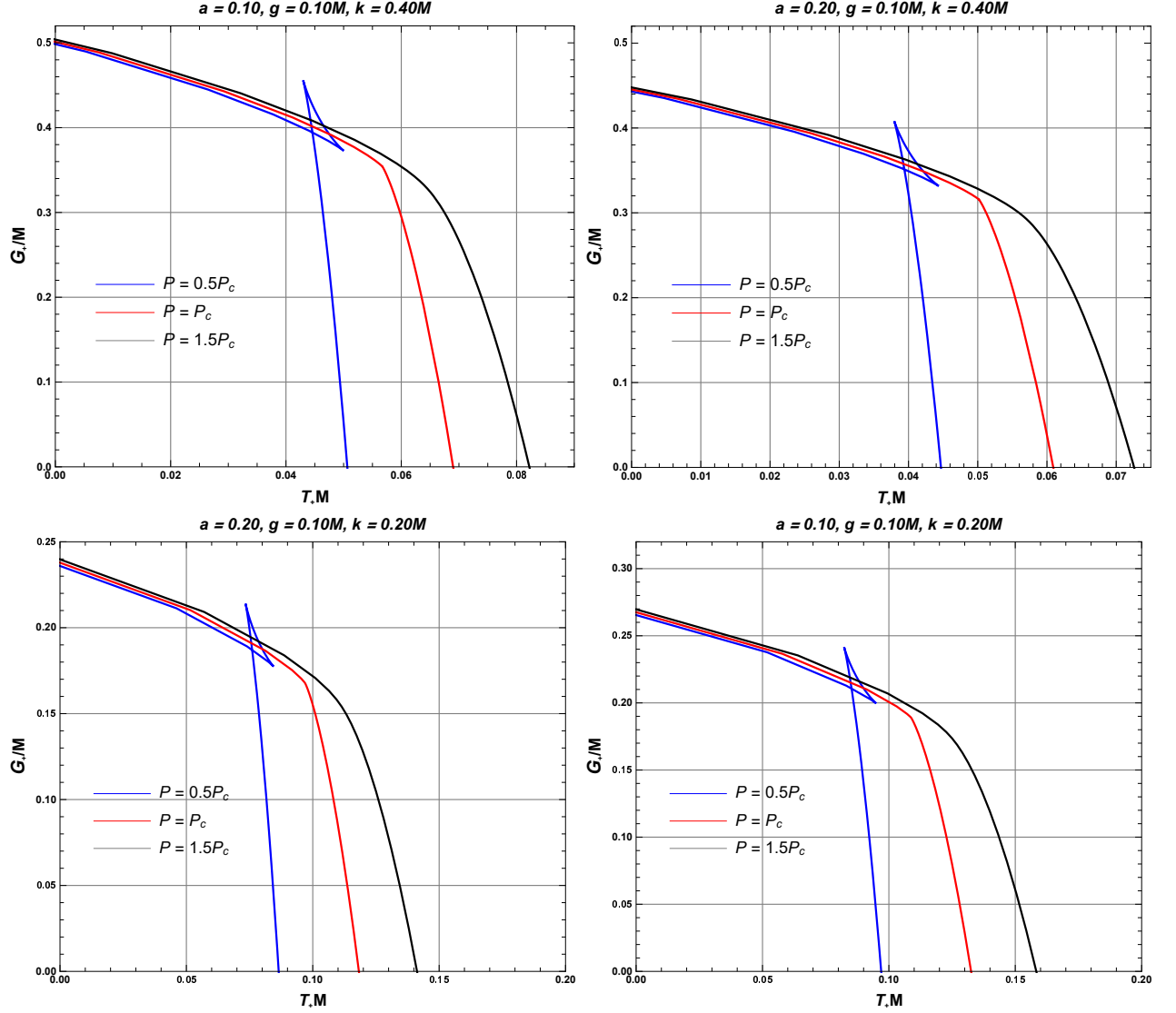


Figure 9. Plot of Gibbs free energy, G_+ versus temperature, T_+ of 4D NLED black hole in a CS for different value of k , g and a around the corresponding critical pressure, P_c .

tail exists for pressure, $P_+ < P_c$, which indicates the first order phase transition and the second order phase transition occurs for pressure, $P_+ = P_c$ in this black hole thermodynamic system.

5 Results and Conclusions

In this work, we have obtained a regular black hole solution in the context of general relativity coupled to NLED sources in the presence of CS in $4D$ AdS spacetime. The resulting solution is characterised by a cloud of string parameters, magnetic charge and deviation parameters, which at most have both Cauchy and event horizons. In the absence of these parameters, this solution corresponds to that of Schwarzschild black hole in AdS spacetime. We have investigated its thermodynamic properties both numerically and graphically. Its stability has been studied by observing heat capacity behaviour and Gibbs free energy. Ultimately, its $P - v$ criticality phenomena have been analysed based on the thermodynamics of the VdW fluid system.

The size of the black hole (event horizon) increases with the increase in the value of the cloud of string parameters. Still, it decreases with the increase in the value of magnetic charge or deviation parameters. Also, these parameters have critical values for which only the event horizon survives. Beyond this limit of parameters, no horizon has been found for this black hole, i.e., the existence of the black hole fades away. Furthermore, we have discussed this black hole's thermodynamics by deriving its mass's expression, Hawking temperature and entropy at the event horizon regarding black hole parameters. The mass of the black hole increases with the increase in values of the magnetic charge or deviation parameters. Still, it decreases with the increase in the value of the CS parameter. On the Hawking temperature, the effect of magnetic charge, deviation parameter or CS parameter is more significant for small black hole regions, where the temperature first increases to a maximum value for a particular horizon radius and then coincides with that of Schwarzschild black hole temperature in large black holes region. Further, we observed that the maximum temperature decreases and shifts towards the area of an enormous horizon radius as the value of these parameters increases. We have noticed that the black hole solution follows the first law of thermodynamics for the fixed value of the magnetic charge. Hence, the black hole's entropy is independent of the cloud of string parameters and follows the usual entropy area law only in the modified first law of thermodynamics. Graphically, it has been observed that the entropy of the black hole has increased with the value of the deviation parameter while it has the opposite variation for magnetic charge.

This black hole's local and global stability has been analysed by investigating the nature of heat capacity and Gibbs free energy, which is dependent on black hole parameters. The heat capacity flip sign at some particular horizon radius resembles the second-order phase transition between unstable and stable phases of the black hole when it changes size from more minor to larger or vice versa. As the values of magnetic charge, deviation parameter, and CS parameters increase, the unstable region of a black hole (negative heat capacity) reduces, allowing the black hole to be thermodynamically stable for NLED sources in the

presence of a CS. The Gibbs free energy analysis has confirmed the existence of local minimum and local maximum where the heat capacity flips its sign. Hence, it provides the theory of the usual Hawking-Page phase transition of the black hole. Further, it has been observed that as the values of parameters increase, the region between the local minimum and local maximum decreases; hence, similar to the case of specific heat capacity, the stability region of the NLED black hole increases in the presence of CS. The $P-v$ criticality of this black hole based on VdW fluid has also been studied. It was found that the critical values significantly depend on the string parameter, magnetic charge, and deviation parameters. The critical pressure and temperature decrease with the increase in the values of these parameters. It has been found that the critical horizon radius and, hence, specific volume increases with an increase in magnetic charge or deviation parameter. The universal compressibility ratio increases with an increase in the value of magnetic charge but decreases with an increase in the value of the deviation parameter. Both specific volume and universal compressibility ratio are independent of a CS parameter. The universal compressibility ratio is equivalent to that of the VdW fluid. Now, to glimpse into the phase structure of its thermodynamic system, the variation of Gibbs energy with temperature near critical pressure has been analysed graphically with the variation of the magnetic charge, deviation parameter and CS parameter. Here, we have observed a characteristic swallow tail for pressure less than its critical value, which indicates the first-order phase transition. After the critical pressure of this black hole thermodynamic system, a second-order phase transition has been observed.

The main achievement of this work is to show that the thermodynamic properties and stability nature of black holes are affected by the parameters of NLED sources and CS in modified gravity. It would be exciting and challenging to focus on the properties of this black hole on higher dimensional solutions. A straightforward extension of our work is to study the black hole shadow problem, which becomes vital after its observational evidence, and the effects of correction due to thermal fluctuations, black bounces, etc, for these black hole solutions. It would also be interesting to analyse the properties of these black holes coupled with the sources of different forms of modified gravity like $f(R)$ gravity, $f(R, \phi)$ gravity, $f(T)$ gravity, $f(\mathcal{G})$ gravity, Einstein-Gauss-Bonnet gravity, Yang-Mills fields, Hořava-Lifshitz gravity and so on. These will be the subject of future investigation.

Acknowledgement

This research was funded by the Science Committee of the Ministry of Science and Higher Education of the Republic of Kazakhstan (Grant No. AP22682760). DVS would like to thank DST-SERB for project no. EEQ/2022/000824.

References

- [1] H. Stephani, D. Kramer, M. MacCallum, C. Hoenselaers, and E. Herlt, *Exact solutions of Einstein's field equations*. Cambridge university press, 2009.
- [2] O. C. Stoica *et al.*, “The geometry of black hole singularities,” *Advances in High Energy Physics*, vol. 2014, 2014.
- [3] J. M. Bardeen, “Proceedings of the International Conference GR5,” 1968.
- [4] E. Ayón-Beato and A. Garcia, “The Bardeen model as a nonlinear magnetic monopole,” *Physics Letters B*, vol. 493, no. 1-2, pp. 149–152, 2000.
- [5] E. Ayon-Beato and A. Garcia, “New regular black hole solution from nonlinear electrodynamics,” *Physics Letters B*, vol. 464, no. 1-2, pp. 25–29, 1999.
- [6] E. Ayon-Beato and A. Garcia, “Regular black hole in general relativity coupled to nonlinear electrodynamics,” *Physical review letters*, vol. 80, no. 23, p. 5056, 1998.
- [7] O. Zaslavskii, “Regular black holes and energy conditions,” *Physics Letters B*, vol. 688, no. 4-5, pp. 278–280, 2010.
- [8] I. Dymnikova, “Vacuum nonsingular black hole,” *General relativity and gravitation*, vol. 24, pp. 235–242, 1992.
- [9] I. Dymnikova, “De Sitter-Schwarzschild black hole: Its particlelike core and thermodynamical properties,” *International Journal of Modern Physics D*, vol. 5, no. 05, pp. 529–540, 1996.
- [10] I. Dymnikova, “Spherically symmetric space–time with regular de Sitter center,” *International Journal of Modern Physics D*, vol. 12, no. 06, pp. 1015–1034, 2003.
- [11] S. A. Hayward, “Formation and evaporation of nonsingular black holes,” *Physical review letters*, vol. 96, no. 3, p. 031103, 2006.
- [12] K. A. Bronnikov, “Regular magnetic black holes and monopoles from nonlinear electrodynamics,” *Physical Review D*, vol. 63, no. 4, p. 044005, 2001.
- [13] K. A. Bronnikov, “Comment on “Construction of regular black holes in general relativity”,” *Physical Review D*, vol. 96, no. 12, p. 128501, 2017.
- [14] M. E. Rodrigues and M. V. d. S. Silva, “Bardeen regular black hole with an electric source,” *Journal of Cosmology and Astroparticle Physics*, vol. 2018, no. 06, p. 025, 2018.
- [15] R. Abbott, T. Abbott, S. Abraham, F. Acernese, K. Ackley, A. Adams, C. Adams, R. Adhikari, V. Adya, C. Affeldt, *et al.*, “GWTC-2: compact binary coalescences observed by LIGO and Virgo during the first half of the third observing run,” *Physical Review X*, vol. 11, no. 2, p. 021053, 2021.
- [16] K. Jafarzade, M. K. Zangeneh, and F. S. Lobo, “Shadow, deflection angle and quasinormal modes of Born-Infeld charged black holes,” *Journal of Cosmology and Astroparticle Physics*,

- vol. 2021, no. 04, p. 008, 2021.
- [17] R. Singh, B. Singh, B. Gupta, and S. Sachan, “Thermodynamic properties of Bardeen black holes in dRGT massive gravity,” *Canadian Journal of Physics*, vol. 100, no. 1, pp. 39–47, 2022.
 - [18] A. Belhaj, L. Chakhchi, H. El Moumni, J. Khalloufi, and K. Masmar, “Thermal image and phase transitions of charged AdS black holes using shadow analysis,” *International Journal of Modern Physics A*, vol. 35, no. 27, p. 2050170, 2020.
 - [19] B. E. Panah, K. Jafarzade, and S. Hendi, “Charged 4D Einstein-Gauss-Bonnet-AdS black holes: Shadow, energy emission, deflection angle and heat engine,” *Nuclear Physics B*, vol. 961, p. 115269, 2020.
 - [20] D. V. Singh, A. Shukla, and S. Upadhyay, “Quasinormal modes, shadow and thermodynamics of black holes coupled with nonlinear electrodynamics and cloud of strings,” *Annals of Physics*, vol. 447, p. 169157, 2022.
 - [21] D. L. Wiltshire, “Black holes in string-generated gravity models,” *Physical Review D*, vol. 38, no. 8, p. 2445, 1988.
 - [22] T. Tamaki and T. Torii, “Gravitating BIon and BIon black hole with a dilaton,” *Physical Review D*, vol. 62, no. 6, p. 061501, 2000.
 - [23] N. Bretón, “Born-Infeld black hole in the isolated horizon framework,” *Physical Review D*, vol. 67, no. 12, p. 124004, 2003.
 - [24] S. Fernando and D. Krug, “Charged black hole solutions in Einstein-Born-Infeld gravity with a cosmological constant,” *General Relativity and Gravitation*, vol. 35, pp. 129–137, 2003.
 - [25] D. V. Singh, S. G. Ghosh, and S. D. Maharaj, “Exact nonsingular black holes and thermodynamics,” *Nucl. Phys. B*, vol. 981, p. 115854, 2022.
 - [26] J. Sadeghi, M. A. S. Afshar, S. Noori Gashti, and M. R. Alipour, “Topology of Hayward-AdS black hole thermodynamics,” *Phys. Scripta*, vol. 99, no. 2, p. 025003, 2024.
 - [27] Z. Luo, H. Yu, S. Cao, and J. Li, “Shadow thermodynamics of the Hayward-AdS black hole*,” *Chin. Phys. C*, vol. 47, no. 6, p. 065102, 2023.
 - [28] B. K. Vishvakarma, D. V. Singh, and S. Siwach, “Parameter estimation of the Bardeen-Kerr black hole in cloud of strings using shadow analysis,” *Phys. Scripta*, vol. 99, no. 2, p. 025022, 2024.
 - [29] B. K. Vishvakarma, D. V. Singh, and S. Siwach, “Shadows and quasinormal modes of the Bardeen black hole in cloud of strings,” *Eur. Phys. J. Plus*, vol. 138, no. 6, p. 536, 2023.
 - [30] B. K. Singh, R. P. Singh, and D. V. Singh, “ $P - v$ criticality, phase structure and extended thermodynamics of AdS ABG black holes,” *Eur. Phys. J. Plus*, vol. 136, no. 5, p. 575, 2021.
 - [31] B. K. Singh, R. P. Singh, and D. V. Singh, “Extended phase space thermodynamics of

- Bardeen black hole in massive gravity,” *Eur. Phys. J. Plus*, vol. 135, no. 10, p. 862, 2020.
- [32] S. G. Ghosh, D. V. Singh, and S. D. Maharaj, “Regular black holes in Einstein-Gauss-Bonnet gravity,” *Phys. Rev. D*, vol. 97, no. 10, p. 104050, 2018.
- [33] P. S. Letelier, “Clouds of strings in general relativity,” *Physical Review D*, vol. 20, no. 6, p. 1294, 1979.
- [34] P. S. Letelier, “Fluids of strings in general relativity,” *Nuovo Cimento B*, vol. 63, pp. 519–528, 1981.
- [35] P. S. Letelier, “String cosmologies,” *Physical review D*, vol. 28, no. 10, p. 2414, 1983.
- [36] A. Ganguly, S. G. Ghosh, and S. D. Maharaj, “Accretion onto a black hole in a string cloud background,” *Physical Review D*, vol. 90, no. 6, p. 064037, 2014.
- [37] J. d. M. Toledo and V. Bezerra, “Black holes with cloud of strings and quintessence in Lovelock gravity,” *The European Physical Journal C*, vol. 78, pp. 1–12, 2018.
- [38] K. Bronnikov, S.-W. Kim, and M. Skvortsova, “The Birkhoff theorem and string clouds,” *Classical and Quantum Gravity*, vol. 33, no. 19, p. 195006, 2016.
- [39] J. d. M. Toledo and V. Bezerra, “The Reissner–Nordström black hole surrounded by quintessence and a cloud of strings: thermodynamics and quasinormal modes,” *International Journal of Modern Physics D*, vol. 28, no. 01, p. 1950023, 2019.
- [40] S. H. Mazharimousavi and M. Halilsoy, “Cloud of strings as source in $2 + 1$ -dimensional $f(R) = R^n$ gravity,” *The European Physical Journal C*, vol. 76, pp. 1–5, 2016.
- [41] J. M. Graça, G. I. Salako, and V. B. Bezerra, “Quasinormal modes of a black hole with a cloud of strings in Einstein–Gauss–Bonnet gravity,” *International Journal of Modern Physics D*, vol. 26, no. 10, p. 1750113, 2017.
- [42] D. Barbosa and V. Bezerra, “On the rotating Letelier spacetime,” *General Relativity and Gravitation*, vol. 48, pp. 1–11, 2016.
- [43] M. Chabab and S. Iraoui, “Thermodynamic criticality of d-dimensional charged AdS black holes surrounded by quintessence with a cloud of strings background,” *General Relativity and Gravitation*, vol. 52, pp. 1–22, 2020.
- [44] E. Herscovich and M. G. Richarte, “Black holes in Einstein–Gauss–Bonnet gravity with a string cloud background,” *Physics Letters B*, vol. 689, no. 4-5, pp. 192–200, 2010.
- [45] X.-C. Cai and Y.-G. Miao, “Quasinormal modes and spectroscopy of a Schwarzschild black hole surrounded by a cloud of strings in Rastall gravity,” *Physical Review D*, vol. 101, no. 10, p. 104023, 2020.
- [46] S. G. Ghosh, U. Papnoi, and S. D. Maharaj, “Cloud of strings in third order Lovelock gravity,” *Physical Review D*, vol. 90, no. 4, p. 044068, 2014.
- [47] D. V. Singh, S. G. Ghosh, and S. D. Maharaj, “Clouds of strings in $4D$

- Einstein–Gauss–Bonnet black holes,” *Phys. Dark Univ.*, vol. 30, p. 100730, 2020.
- [48] Y. Yang, D. Liu, A. Övgün, G. Lambiase, and Z.-W. Long, “Rotating black hole mimicker surrounded by the string cloud,” *Phys. Rev. D*, vol. 109, no. 2, p. 024002, 2024.
- [49] Y. Yang, D. Liu, Z. Xu, and Z.-W. Long, “Ringing and echoes from black bounces surrounded by the string cloud,” *Eur. Phys. J. C*, vol. 83, no. 3, p. 217, 2023.
- [50] J. D. Bekenstein, “Black holes and the second law,” *Lett. Nuovo Cim.*, vol. 4, pp. 737–740, 1972.
- [51] J. D. Bekenstein, “Black holes and entropy,” *Phys. Rev. D*, vol. 7, pp. 2333–2346, Apr 1973.
- [52] S. W. Hawking, “Black holes and thermodynamics,” *Phys. Rev. D*, vol. 13, pp. 191–197, Jan 1976.
- [53] A. Strominger and C. Vafa, “Microscopic origin of the Bekenstein-Hawking entropy,” *Phys. Lett. B*, vol. 379, pp. 99–104, 1996.
- [54] A. Ashtekar, J. Baez, A. Corichi, and K. Krasnov, “Quantum geometry and black hole entropy,” *Phys. Rev. Lett.*, vol. 80, pp. 904–907, 1998.
- [55] S. Chougule, S. Upadhyay, H. K. Sudhanshu, and S. Kumar, “Hawking radiation as tunnelling from dilatonic BTZ black hole,” *JHAP*, vol. 3, no. 3, pp. 45–52, 2023.
- [56] B. Pourhassan, H. Farahani, F. Kazemian, I. Sakallı, S. Upadhyay, and D. V. Singh, “Non-perturbative correction on the black hole geometry,” *Phys. Dark Univ.*, vol. 44, p. 101444, 2024.
- [57] H. K. Sudhanshu, D. V. Singh, S. Bekov, K. Myrzakulov, and S. Upadhyay, “P–v criticality and Joule–Thomson expansion in corrected thermodynamics of conformally dressed (2+1)D AdS black hole,” *Int. J. Mod. Phys. A*, vol. 38, no. 29n30, p. 2350165, 2023.
- [58] J. Kumar, S. Upadhyay, and H. K. Sudhanshu, “Small black string thermodynamics,” *Phys. Scripta*, vol. 98, no. 9, p. 095306, 2023.
- [59] S. Upadhyay, N. ul islam, and P. A. Ganai, “A modified thermodynamics of rotating and charged BTZ black hole,” *JHAP*, vol. 2, no. 1, pp. 25–48, 2022.
- [60] S. Upadhyay and B. Pourhassan, “Logarithmic corrected Van der Waals black holes in higher dimensional AdS space,” *PTEP*, vol. 2019, no. 1, p. 013B03, 2019.
- [61] M.-Y. Zhang, H. Chen, H. Hassanabadi, Z.-W. Long, and H. Yang, “Joule-Thomson expansion of charged dilatonic black holes,” *Chin. Phys. C*, vol. 47, no. 4, p. 045101, 2023.
- [62] M.-Y. Zhang, H. Chen, H. Hassanabadi, Z.-W. Long, and H. Yang, “Topology of nonlinearly charged black hole chemistry via massive gravity,” *Eur. Phys. J. C*, vol. 83, no. 8, p. 773, 2023.
- [63] M.-Y. Zhang, H. Chen, H. Hassanabadi, Z.-W. Long, and H. Yang, “Critical behavior and Joule-Thomson expansion of charged AdS black holes surrounded by exotic fluid with

- modified Chaplygin equation of state*,” *Chin. Phys. C*, vol. 48, no. 6, p. 065101, 2024.
- [64] H. Chen, M.-Y. Zhang, H. Hassanabadi, B. C. Lütfüoğlu, and Z.-W. Long, “Topology of dyonic AdS black holes with quasitopological electromagnetism in Einstein-Gauss-Bonnet gravity,” 3 2024.
- [65] H. Chen, M.-Y. Zhang, H. Hassanabadi, and Z.-W. Long, “Thermodynamic topology of Phantom AdS Black Holes in Massive Gravity,” 4 2024.
- [66] J. L. Synge, “Relativity: the general theory,” 1960.
- [67] M. E. Rodrigues and M. V. d. S. Silva, “Embedding regular black holes and black bounces in a cloud of strings,” *Physical Review D*, vol. 106, no. 8, p. 084016, 2022.
- [68] M. E. Rodrigues and H. A. Vieira, “Bardeen solution with a cloud of strings,” *Phys. Rev. D*, vol. 106, no. 8, p. 084015, 2022.
- [69] M. E. Rodrigues, M. V. de S. Silva, and H. A. Vieira, “Bardeen-Kiselev black hole with a cosmological constant,” *Phys. Rev. D*, vol. 105, no. 8, p. 084043, 2022.
- [70] R. M. Wald, “Black hole entropy is the Noether charge,” *Physical Review D*, vol. 48, no. 8, p. R3427, 1993.
- [71] M.-S. Ma and R. Zhao, “Corrected form of the first law of thermodynamics for regular black holes,” *Classical and Quantum Gravity*, vol. 31, no. 24, p. 245014, 2014.
- [72] N. Goldenfeld, *Lectures on phase transitions and the renormalization group*. CRC Press, 2018.